Calculating Slow-Motional Electron Paramagnetic Resonance Spectra from Molecular Dynamics Using a Diffusion Operator Approach

David E. Budil,*,† Kenneth L. Sale,‡,§ Khaled A. Khairy,†,‡,# and Peter G. Fajer‡

Department of Chemistry and Chemical Biology, Northeastern University, Boston Massachusetts 02115, and Department of Biological Science, Institute of Molecular Biophysics, Florida State University, Tallahassee, Florida 32310

Received: August 22, 2005; In Final Form: December 8, 2005

A number of groups have utilized molecular dynamics (MD) to calculate slow-motional electron paramagnetic resonance (EPR) spectra of spin labels attached to biomolecules. Nearly all such calculations have been based on some variant of the trajectory method introduced by Robinson, Slutsky and Auteri (*J. Chem. Phys.* **1992**, *96*, 2609−2616). Here we present an alternative approach that is specifically adapted to the diffusion operator-based stochastic Liouville equation (SLE) formalism that is also widely used to calculate slow-motional EPR line shapes. Specifically, the method utilizes MD trajectories to derive diffusion parameters such as the rotational diffusion tensor, diffusion tilt angles, and expansion coefficients of the orienting potential, which are then used as direct inputs to the SLE line shape program. This approach leads to a considerable improvement in computational efficiency over trajectory-based methods, particularly for high frequency, high field EPR. It also provides a basis for deconvoluting the effects of local spin label motion and overall motion of the labeled molecule or domain: once the local motion has been characterized by this approach, the label diffusion parameters may be used in conjunction with line shape analysis at lower EPR frequencies to characterize global motions. The method is validated by comparison of the MD predicted line shapes to experimental high frequency (250 GHz) EPR spectra.

Introduction

Site directed spin labeling coupled with electron paramagnetic resonance spectroscopy (SDSL-EPR) provides a powerful technique for the analysis of protein orientation and of protein motions on the nanosecond to microsecond times scales. However, interpretation of EPR spectra in terms of protein orientation and dynamics is often confounded by librational motion of the spin label with respect to the biomolecule. The EPR spectrum, which measures probe behavior, is a convolution of protein orientation and motion with respect to the macromolecular complex and of spin label orientation and motion with respect to the protein to which it is attached. When both motions either fall into the slow-motion region or occur over a broad dynamic range, it becomes necessary to account for them explicitly. Experimentally, one way of discriminating between probe and overall motion is to observe the spin label spectrum by high frequency (HF) EPR, where the slower tumbling and conformational motions of the protein are effectively "frozen out" and the spectrum is sensitive to the details of spin label diffusion within the local environment of the label.[1] Because of its high spectral resolution, HF EPR also allows the local probe motions and ordering to be characterized in much greater detail than is possible by EPR at conventional frequencies. Once the spin label motion has been completely characterized using HF EPR, detailed information on overall or domain motion of the protein may in principle be obtained by EPR at lower frequencies.

Probe motion can also be accounted for using computational techniques such as molecular dynamics (MD). Most of the MD studies that have been reported to date utilize some variant of the Brownian dynamics (BD) method pioneered by Robinson et al.[2] to simulate the EPR spectrum. In this method, a Brownian trajectory of molecular orientations is used to generate the time evolution of the magnetization operator, which is Fourier transformed to obtain the cw-EPR signal. The BD method was applied to protein systems by Steinhoff and co-workers,[3,4] who used MD trajectories to define a mean force potential, from which single-particle BD trajectories and thence EPR spectra were calculated. Westlund and co-workers developed an alternative method for solving the time evolution of magnetization directly from MD trajectories using an algorithm designed to conserve the norm of the time propagator at every step of the trajectory.[5,6]

Although several groups have calculated EPR spectra from MD trajectories, only Steinhoff and co-workers have compared their calculations directly to experimental spectra.[7,8] These authors demonstrated overall qualitative agreement with X-band spectra from spin-labeled bacteriorhodopsin (BR)[8] and MD calculations on either BR itself or a trileucine fragment.[7] A more rigorous test of the MD method is comparison with experimental high frequency EPR spectra because of their greater sensitivity to motion on the fast time scale of the label motions. However, the only reported attempt to simulate HF-EPR results[9] failed to reproduce 250 GHz spectra of spin-labeled T4 lysozyme from 55 to 60 ns trajectories, concluding that much longer sampling

* To whom correspondence should be addressed. E-mail: D.Budil@neu.edu.

† Northeastern University.

‡ Florida State University.

§ Present address: Biosystems Research Department, Sandia National Laboratories, Livermore, CA 94551-9292.

Present address: Max Planck Institute for Molecular and Cell Biology and Genetics, 01307 Dresden, Germany.

10.1021/jp054738k CCC: $33.50
Published on Web 02/18/2006

and more extensive averaging over initial conditions will be required to obtain reliable HF-EPR simulation.

An attractive and computationally efficient alternative to trajectory-based EPR simulations is to represent spin probe motion in diffusion operator form and solve the stochastic Liouville equation (SLE) as an eigenfunction expansion.[10−12] In this method, the rotational diffusion of the spin probe is restricted by an orienting potential, which is expanded in terms of the same eigenfunctions. Freed and co-workers have extended their original model to describe combined probe and protein motion in terms of a slowly relaxing local structure (SRLS),[13] which models the combined fast anisotropic probe motion with slow, isotropic macromolecular tumbling.

In this work, we introduce a new method for MD-based simulation of EPR spectra that differs fundamentally from previously reported approaches. The basic strategy is to utilize the MD trajectory to derive diffusion operator parameters such as the rotational diffusion tensor and orienting potential expansion coefficients, which are then used as input parameters for the SLE line shape calculation. This approach combines the speed advantage of SLE methods to generate the EPR spectra with the fidelity of the MD calculations to reproduce or predict the local potential experienced by the spin label.

To test this method, we also demonstrate a direct comparison of HF-EPR spectra predicted by MD with experimental spectra from the literature. Because only a limited number of spectra from spin-labeled proteins are available at very high field; we selected the protein T4 lysozyme as a model system, for which 250 GHz data have been published by Barnes et al.[1]

Methods

Spin Label Topologies and Force Field Parameters. The crystal structure of T4 lysozyme (3LZM) (MW ∼ 14 kD)[14] was used as the model structure for all simulations. Serine 44 and glutamine 69 were separately changed to a spin label ((1-oxyl-2,2,5,5-tetramethylpyrroline-3-methyl)methanethiosulfonate; MTSSL) modified cysteine residue (CMTS; Figure 1) using the Insight II Biopolymer module. Spin label structures were built using the Insight II Builder module and stored as PDB formatted files. To accommodate the spin-labeled cysteine in the CHARMM19 extended atom force field, two new atom types, NN and ON, were added to represent the nitroxide nitrogen and nitroxide oxygen, respectively. Force field parameters were derived and added as previously described.[15] The addition of these atom types allows for the correct parametrization of dihedral and improper angles necessary to mimic the nitroxide moiety topology of the X-ray structures determined by Lajzerowicz-Bonneteau[16] and the ab initio models of Barone et al.[17,18] Partial charges were determined using a set of rules described by Barone et al.[17,18] Following extensive energy minimization, all bond lengths were within 0.05 Å and all bond angles were within 5° of their crystal structure values for both five and six member nitroxide rings.

The structure of MTSSL modified cysteine, its torsional degrees of freedom, atom names, CHARMM19 atom types and partial charges are shown in Figure 1. The spin label was docked to the cysteine using disulfide bond parameters: an S−S bond length of ∼2.0 Å and a C−S−S bond angle of ∼100°. The MTSSL-modified cysteine structure was added to the Insight II library of amino acids, used to mutate any protein residue to CMTS using the "mutate" command of the Builder module. For the present study, the spin labels were attached at sites 44 and 69, corresponding to the two sites for which experimental

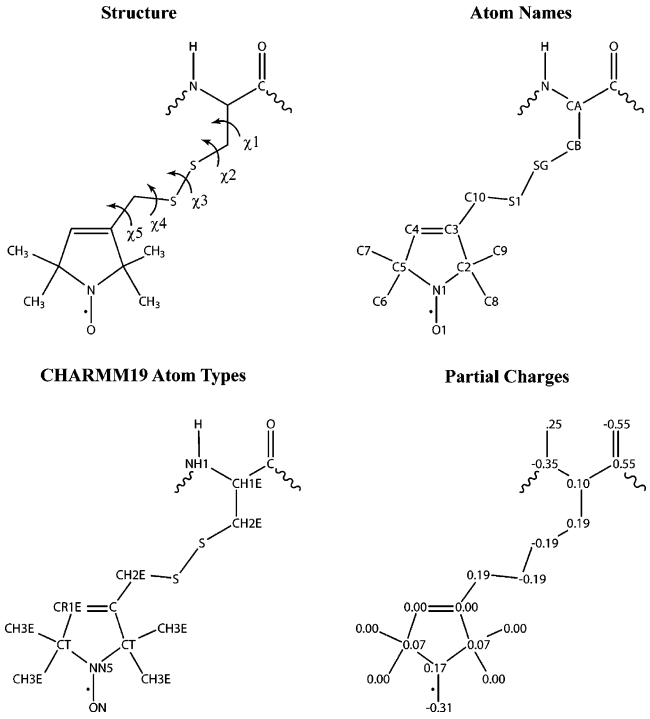

Figure 1. Structure of cysteine modified with the MTSSL spin label (CMTS), showing the side-chain dihedral angles, CHARMm atom types, atom names, and partial charges.

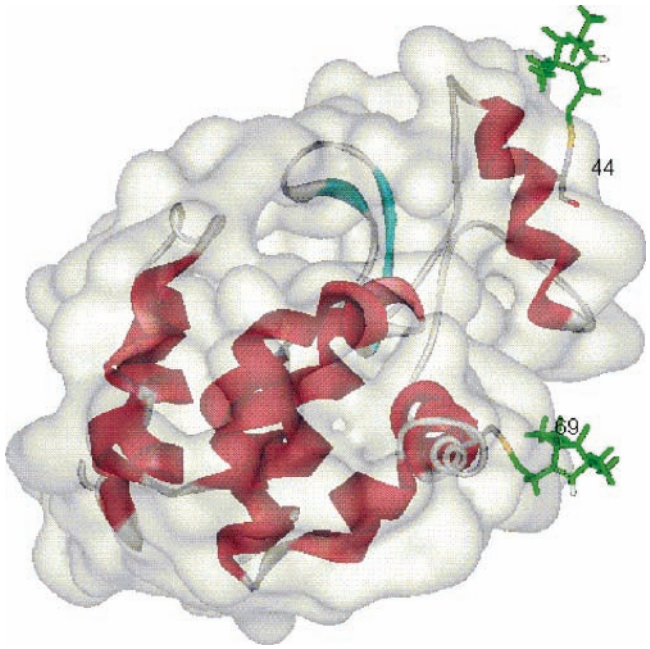

Figure 2. Structure and surface of T4 lysozyme showing MTSSL attached at sites 44 and 69.

high-field EPR data are available.[1] The position of the labels at these two sites relative to the surface of the protein is shown in Figure 2.

Molecular Modeling. All energy calculations were performed with the CHARMM19 extended atom force field using a distance dependent dielectric as an implicit solvent model.[19] Energy calculations were confined to the interactions between the spin label and amino acid residues within a 15 Å sphere of the label. The CHARMm switching function was used to smooth the transition over a cutoff range of 13 to 15 Å. Conformational searching of the torsional space of the docked spin label over the five bonds tethering the nitroxide ring to the cysteine (Figure

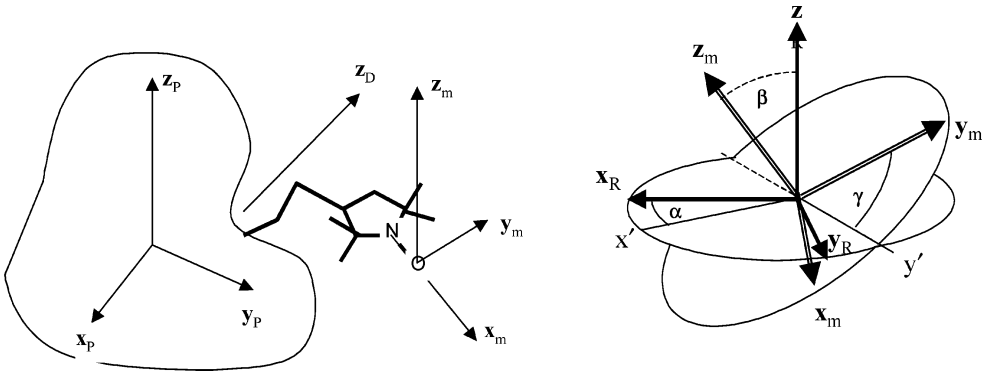

Figure 3. Definition of coordinate systems used in this work. x_P, y_P, z_P: protein-fixed axis system. z_D: director axis. x_M, y_M, z_M: magnetic axes, fixed relative to the nitroxide atomic coordinates. x_R, y_R, z_R: rotational diffusion principal axes, which are related to the magnetic axes by the Euler angles (α, β, γ) as shown on the right-hand side.

1) was performed using a Monte Carlo minimization algorithm[20−22] developed and validated for spin label modified side chains.[15] Briefly, the search consists of iterations in which a randomly chosen torsion angle is set to a random value followed by energy minimization using the adopted basis Newton Raphson (ABNR) algorithm. Extensive conformational searches of the starting point of MD simulations is necessary to ensure that the correct conformational space of the label is being explored by MD.

Molecular dynamics calculations in the microcanonical (NVT) ensemble were used to simulate the librational motion and dynamic properties of the spin label in the protein matrix. The equations of motion were integrated using the Verlet leapfrog method with a 2 fs time step. The system was gradually heated to a temperature of 300 K over 6000 steps (12 ps) and MD production runs were carried out for 1 ns at 300 K without velocity rescaling. The coordinates were corrected for global translation and rotation every 200 fs so that the MD trajectory reflected only the spin label motion relative to the protein. During the production run, coordinates of the spin label and energies were sampled every 200 fs.

Definition of Axis Systems. Before discussing the different parameters used in the diffusion operator SLE formalism, it is necessary to define a number of different coordinate systems, depicted in Figure 3. The first is the coordinate system in which the MD calculation is carried out. Because the overall orientation of the protein is fixed in this system, we will refer to it as the protein frame ($\mathbf{x}_P$, $\mathbf{y}_P$, $\mathbf{z}_P$). The second frame of interest is the director frame ($\mathbf{x}_D$, $\mathbf{y}_D$, $\mathbf{z}_D$), which is fixed in the protein frame. The $\mathbf{z}_D$ axis is used to define the energy potential that imposes orientational order on the probe molecule.

The magnetic frame ($\mathbf{x}_M$, $\mathbf{y}_M$, $\mathbf{z}_M$) is fixed relative to the structure of the nitroxide label and may be defined using the atomic coordinates of the nitroxide moiety as follows: $\mathbf{x}_M$ is the unit vector along the N−O bond direction $\overrightarrow{N_1O_1}$ (where the subscripts are derived from the atom labels defined in Figure 1), and $\mathbf{z}_M$ is taken to be the unit vector along axis of the nitrogen p-orbital. This direction is calculated as the unit vector along the direction $\overrightarrow{C_2N_1} \times \overrightarrow{N_1O_1} + \overrightarrow{N_1O_1} \times \overrightarrow{N_1C_5}$ to ensure that it remains perpendicular to $\mathbf{x}_M$. Finally, $\mathbf{y}_M$ is obtained as $\mathbf{z}_M \times \mathbf{x}_M$.

Another important frame is the principal axis system of the rotational diffusion tensor, or rotational diffusion frame ($\mathbf{x}_R$, $\mathbf{y}_R$, $\mathbf{z}_R$), which is fixed relative to the magnetic frame. The relative orientations of the diffusion and magnetic axes are specified by the diffusion tilt angles $\Omega_D = (\alpha_D, \beta_D, \gamma_D)$, which are the Euler angles, of the magnetic axes in the diffusion frame, specified according to the y-convention defined in ref 23 and shown in Figure 3.

Ordering Potential. For diffusion of a probe in a medium with microscopic molecular ordering such as liquid crystals, lipid membranes, polymers, or biopolymers, the tendency of the probe to order may be modeled by a restoring potential $U(\Omega)$, where Ω represents the Euler angles of the diffusion axes in the director frame. The potential function $U(\Omega)$ may be expanded in a series of Wigner rotation functions $\mathbf{D}^L_{MK}(\Omega)$, which for $M = 0$ are proportional to the ordinary spherical harmonics $Y^L_K(\theta,\phi)$, where θ and ϕ are the polar angles of $\mathbf{z}_D$ in the magnetic frame. This expansion may be written

$$U(\theta,\phi) = -k_bT\sum_{L,K}\epsilon^L_K\mathbf{D}^L_{0K}(\theta,\phi) = -\sum_{L,K}c^L_K\mathbf{D}^L_{0K}(\theta,\phi) \quad (1)$$

where the ϵ^L_K coefficients are dimensionless and real-valued, and in general include both positive and negative K indices. In the currently available SLE programs,[10,12] the temperature-scaled coefficients $c^L_K = k_bT\epsilon^L_K$ are used to describe the orienting potential, and are expressed in units of k_bT. Furthermore, the indices L and K are limited to even integers of magnitude less than or equal to 4, and the coefficients are assumed to have the property that $\epsilon^L_K = \epsilon^L_{-K}$; i.e., $U(\Omega)$ is restricted to symmetric combinations of $\mathbf{D}^L_{MK}(\Omega)$ and $\mathbf{D}^L_{M,-K}(\Omega)$. Thus, the summation in eq 1 may be rewritten

$$U(\Omega) = -k_bT\sum_{0<L,K\le 4,\text{even}}c^L_K(\mathbf{D}^L_{0,K}(\Omega) + \mathbf{D}^L_{0,-K}(\Omega)) \quad (2)$$

so that in the summation only the parameters c_0^2, c_2^2, c_0^4, c_2^4, and c_4^4 are included in the EPR line shape calculation. These two restrictions are based on the assumption that the shape of the orienting potential is symmetrical with respect to the director axis, and also that the ordering axes of the spin label coincide with its rotational diffusion axes.

Calculation of Ordering Potential Coefficients. The $U(\Omega)$ function is defined in terms of the orientation of the director axis z_D relative to the diffusion axis system of the spin label. Therefore, the c^L_K potential coefficients may be obtained from the distribution of director orientations that is observed in the diffusion frame over the course of the MD run. This distribution is calculated by constructing a population matrix of the number of times the director axis visits each (θ, ϕ) orientation in the diffusion axis frame. Typically, 41 θ and ϕ values were used to construct the matrix. The population matrix is then used to estimate the orientation probability matrix $P_{MD}(\theta,\phi)$ by normalizing it to the total number of orientations (here the subscript MD is used to identify distributions calculated from MD trajectories).

The orienting potential $U(\theta,\phi)$ may be used to calculate a probability distribution $P_B(\theta,\phi)$ according to the Boltzmann distribution law:

$$P_B(\theta,\phi) = \frac{e^{-U(\theta,\phi)/k_bT}}{Z} = \frac{e^{-U(\theta,\phi)/k_bT}}{\int_\Omega e^{-U(\theta,\phi)/k_bT}} \quad (3)$$

where k_b is the Boltzmann constant, T is temperature and Z is the partition function calculated by integrating over all orientations (θ,ϕ).

To determine the set of potential coefficients c_K^L for the $U(\theta,\phi)$ that best represents $P_{MD}(\theta,\phi)$ according to eq 3, the coefficients are varied in a nonlinear least-squares minimization of the quantity

$$\chi^2 = \sum_{\theta,\phi}(P_{MD}(\theta,\phi) - P_B(\theta,\phi))^2 \quad (4)$$

To automate the nonlinear least-squares analysis, an initial estimate of the potential coefficients may be made using linear least-squares. Because U is a linear function of the spherical harmonics, rewriting eq 3 as a linear least-squares equation:

$$\ln P_{MD}(\theta,\phi) = -U(\theta,\phi)/k_bT - \ln Z = \sum_{L,K} c_K^L D_{0K}^L(\theta,\phi) - \ln Z \quad (5)$$

The coefficients are then obtained by reshaping the $\ln P_{MD}(\theta,\phi)$ matrix and each of the $D_{0K}^L(\theta,\phi)$ function values as column vectors and solving the matrix equation

$$\begin{pmatrix} \ln P_{MD,1} \\ \ln P_{MD,2} \\ \vdots \\ \ln P_{MD,k} \end{pmatrix} = \begin{pmatrix} {D_{00,1}}^2 & {D_{02,1}}^2 & \cdots & {D_{0K,1}}^L & -1 \\ {D_{00,2}}^2 & {D_{02,2}}^2 & \cdots & {D_{0K,2}}^L & -1 \\ \vdots & \vdots & \ddots & \vdots & \vdots \\ {D_{00,k}}^2 & {D_{02,k}}^2 & \cdots & {D_{0K,k}}^L & -1 \end{pmatrix} \begin{pmatrix} {c_0}^2 \\ {c_2}^2 \\ \vdots \\ {c_K}^L \\ Z \end{pmatrix} \quad (6)$$

Orientations for which $P_{MD}(\theta,\phi) = 0$ are not included in the linear least-squares equation.

In principle, these two methods should give equivalent results, because for ergodic trajectories, $\ln P_{MD}(\theta,\phi)$ should be linearly related to $U(\theta,\phi)$. In practice, the coefficients derived by the two methods do differ, with the nonlinear least-squares fit to $P_{MD}(\theta,\phi)$ giving a consistently better fit according to the criterion in eq 4. This may be a consequence of including orientations for which $P_{MD}(\theta,\phi) = 0$ in the nonlinear fit.

Determination of Director and Diffusion Tilt Angles. Because $P_{MD}(\theta,\phi)$ represents the probability of finding the director axis in the rotational diffusion frame, both the director and the rotational diffusion axes must be known before $P_{MD}(\theta,\phi)$ may be calculated. There are a number of ways in which these orientations might be defined from the MD trajectory. We first consider the diffusion axes. Unlike free spin probes, where the principal diffusion axes can be estimated from the hydrodynamic properties of the molecule, the tether of label molecules considerably complicates their diffusive behavior. Although there has been no systematic determination of the rotational diffusion axes of covalently attached nitroxide labels using MD, two groups have estimated the diffusion tilt angles from least-squares analysis of experimental EPR spectra. Columbus et al.[24] have noted that X-band simulations are sensitive only to the β_D angle and obtained best agreement with experiment for $\beta_D = 36°$. Barnes et al.[1] proposed two models for the rotational diffusion tensor using geometric arguments. In the first model, rotations around χ_4 and χ_5 are restricted by steric interactions between the sulfurs and nitroxide ring methyl groups, producing fastest rotation around the z_M axis, corresponding to zero tilt angles. For the second model, in which there is free rotation about the nitroxide tether bonds, they chose the principal diffusion axis as the direction from the C_α carbon of cysteine to C3 of the pyrroline ring (cf. Figure 1), leading to diffusion tilt angles $(\alpha_D, \beta_D, \gamma_D) = (0°, 25°, 36°)$. Reasonable fits to the spectra could be obtained for both of these models, producing different sets of potential coefficients.

There are similar ambiguities regarding the choice of the director axis. In the liquid crystalline and membrane systems for which the SLE line shape calculation was originally designed,[25] the director is clearly defined by the direction of macroscopic alignment of the solvent or membrane. In the case of a tethered spin label at the irregularly shaped surface of a protein, the correct director orientation is not obvious from the molecular structure, and a formal definition of the director is required. A convention that has been used previously in the context of MD analysis[26] is the "mode" of the $\mathbf{z}_R$ orientation, that is, the orientation (θ, ϕ) for which $P_{MD}(\theta,\phi)$ is a maximum. Another possible definition is the average orientation of z_R over the trajectory, which should be the same as the mode for simple, symmetrical distributions. The most rigorous definition of the director is to use the Saupe order matrix and reverse the procedure of Zannoni.[27] Specifically one constructs the Saupe ordering matrix $\mathbf{S}$ of the principal diffusion axis in an arbitrary protein-fixed frame.[28] Explicitly, the elements of $\mathbf{S}$ are

$$S_{ij} = \frac{1}{2}\langle 3\cos\theta_i \cos\theta_j - \delta_{ij}\rangle \quad (7)$$

where δ is the Kronecker delta function, $i, j = \mathbf{x}_P, \mathbf{y}_P, \mathbf{z}_P$, θ_i is the angle between $\mathbf{z}_R$ and the i axis, and the angle brackets denote averaging over a suitable ensemble of molecular orientations, such as the MD trajectory. The matrix $\mathbf{S}$ may then be diagonalized to find the director, which is the axis corresponding to the largest eigenvalue of $\mathbf{S}$.

We note that in all of these possible definitions, the resulting director orientation will depend critically upon which axis is selected as the principal diffusion axis. In practice, we found considerable differences among the directors defined by these various methods, leading to substantial variation in the potential coefficients derived from them.

To avoid potential complications and ambiguities regarding the director and diffusion axis orientations, no a priori assumptions were made about these orientations in our analysis of the MD trajectories. Instead, these orientations were determined directly from the trajectories by optimizing the diffusion tilt angles and the two polar angles describing the director orientation in the protein frame as follows. The angle parameters were searched using the Nelder−Mead downhill simplex method,[29] starting from zero tilt angles and using the average $\mathbf{z}_R$ direction as an initial estimate for the director orientation. At each step of the search, the potential coefficients were determined by the nonlinear least-squares procedure described above and the χ^2 of the fit was calculated according to eq 4. The search of the angle parameters terminated when a global minimum in χ^2 was located.

Results

Starting structures of T4 lysozyme labeled with MTSSL at residue 44 and at 69 were determined by Monte Carlo minimization searches over the spin label torsional space, as

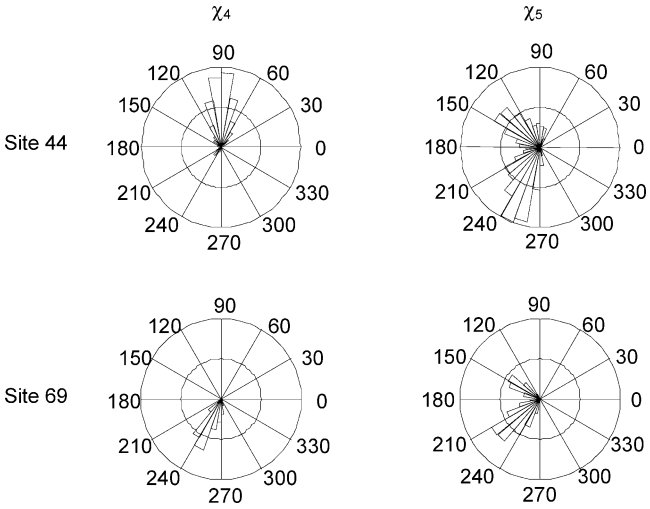

Figure 4. Distribution of torsional angles χ_4 (left) and χ_5 (right) over the MD trajectories calculated for label sites 44 (top) and 69 (bottom) at 300 K.

TABLE 1: Side-Chain Dihedral Angles χ_1 through χ_5 for the 300 K Trajectories of Spin Labels at Two Sites on T4 Lysozyme

site	χ_1	χ_2	χ_3	χ_4	χ_5
44	295 ± 8	228 ± 26	85 ± 10	103 ± 48	188 ± 63
69	295 ± 8	245 ± 17	87 ± 9	248 ± 18	197 ± 41

TABLE 2: Diffusion Tilt Angles (in degrees) Derived from Analysis of MD Trajectories of Nitroxide Labels Attached to Residues 44 and 69 of T4 Lysozyme

label site	α_D	β_D	γ_D
44	0.1	105.3	−0.4
69	−0.2	93.0	−0.1

has been described previously.[15] Figure 2 reveals the likely basis of the restricted motion of MTSSL at both label sites: although the labels are on the surface of the protein, they are constrained both by their covalent linkage to the protein backbone and by local side-chain interactions. The minimized conformations were used as the starting points for 1 ns MD trajectories carried out for each label site.

The MD trajectories of the torsion angles of the label side chain are shown in Figure 4, and tabulated in as the average angle and standard deviation from the average angle calculated over the trajectories for label sites 44 and 69. The pattern of the label dynamics reveals only modest variation around the χ_1, χ_2 and χ_3 torsion angles, whereas the χ_4 and χ_5 torsion angles show larger variation (Figure 4). This is in agreement with X-ray structures of MTSSL labeled T4 lysozyme[30] and an analysis of the motion of a series of MTSSL derivative structures,[24] which also implicated rotations of the χ_4 and χ_5 torsion angles as the major contributors to MTSSL dynamics. The agreement provides a qualitative validation of our choice of the CHARMM19 force field, which includes significant electrostatic and van der Waals contributions (the so-called "1−4" interactions).

Diffusion Tilt Angles. The diffusion tilt angles determined by the procedure described above are given in Table 2, and the directions of the principal rotational diffusion axes are shown graphically with respect to the atomic structure of the label in Figure 5.

For both label sites, the major axis of the spin label rotation, $\mathbf{z}_R$, lies slightly out of the plane of the nitroxide ring, and within about 5−15° from the N−O bond direction. This direction of $\mathbf{z}_R$ is most consistent with a model of rapid rotation around the

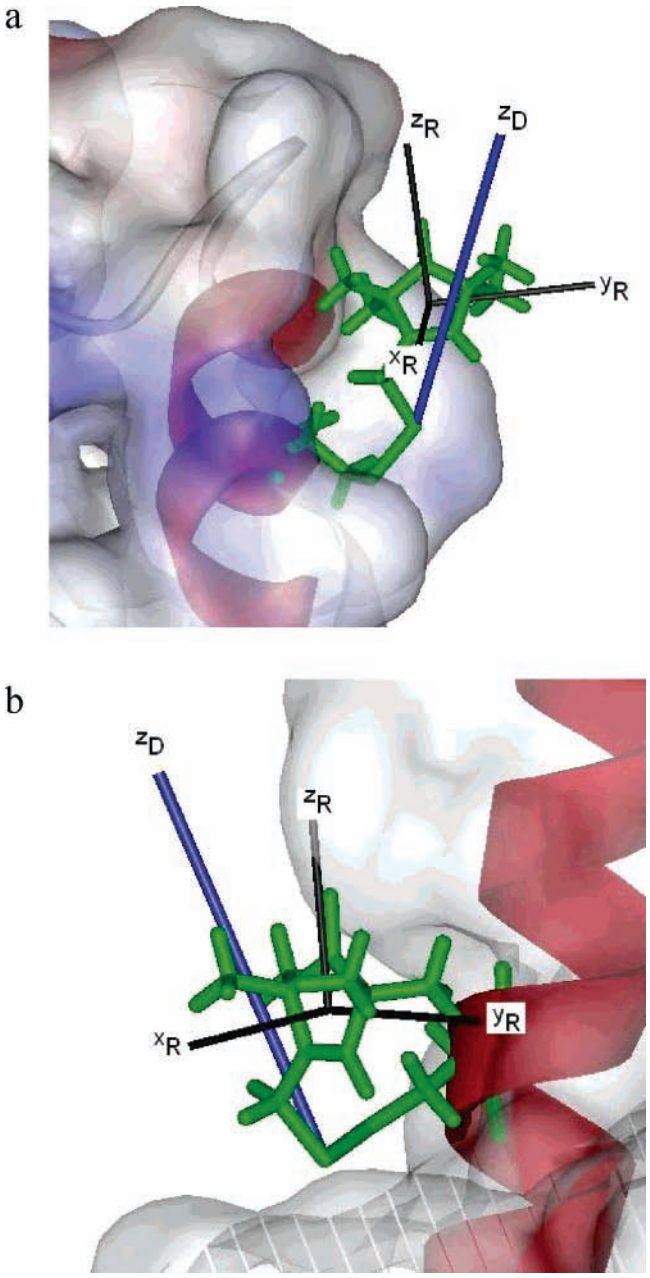

Figure 5. Orientations of principal diffusion axes (x_R, y_R, z_R) and director axis (z_D) relative to molecular structure of the nitroxide label and the T4 lysozyme surface for site (a) 44 and (b) 69.

χ_5 dihedral angle as the major motion of the spin label, and also consistent with the dihedral angle distributions shown in Table 2 and Figure 4. These MD results contrast with the suggestion by Barnes et al.[1] that steric interaction between the sulfur atoms and ring methyl groups may restrict rotation of χ_5 to a range of 20°.

Director Axis. The directors determined from the MD trajectories for each label site are shown relative to the molecular structures of the label plus protein in Figure 5. As this figure shows, the directors are generally more closely related to the orientation of the label tether chain than they are to the shape of the surface of the surrounding protein side chains.

Ordering Potential. The potential coefficients obtained from analysis of the MD trajectories are given for each label sites in Table 3. Figure 6 shows orientation distribution plots of the director axis $\mathbf{z}_D$ in the rotational diffusion frame, $P_{MD}(\theta,\phi)$, of the spin label for label sites 44 and 69, together with the orientation distributions $P_B(\theta,\phi)$ calculated from the optimized

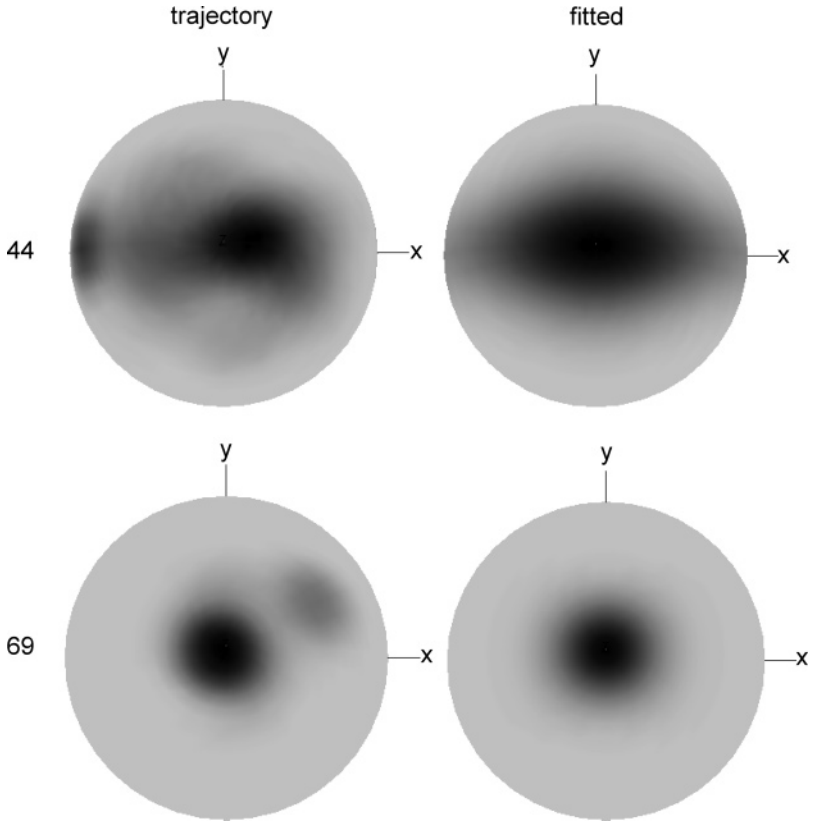

Figure 6. Intensity plots (left) depicting the director axis distribution in the nitroxide diffusion frame, $P_{MD}(\theta,\phi)$, for T4 lysozyme labeled at sites 44 (top) and 69 (bottom) at 300 K Shown at right are distributions corresponding to the best-fit orienting potential parameters, $P_B(\theta,\phi)$ obtained as described in the text.

TABLE 3: Orienting Potential Coefficients (in Units of k_bT at 300 K) Determined from MD Trajectories for MTSSL at Label Sites 44 and 69 on T4 Lysozyme

site	c_0^2	c_2^2	c_0^4	c_2^4	c_4^4
44	2.96 ± 0.29	1.72 ± 0.61	-0.19 ± 0.41	-0.06 ± 0.33	0.80 ± 0.92
69	3.66 ± 0.91	1.80 ± 3.54	1.24 ± 1.12	-0.344 ± 1.38	-1.12 ± 4.64

diffusion tilt angles and potential coefficients obtained from the MD trajectories. By definition, the distributions appear near the $\mathbf{z}_R$ axis of the label. Also shown in Figure 6 are the fits to the P director distribution obtained by the linear least-squares fitting procedure described above.

Table 3 also gives estimated 95% confidence intervals in the potential coefficients obtained from the nonlinear fits to the $P_{MD}(\theta,\phi)$ distributions. These intervals were estimated from the covariance matrix that may be calculated from the curvature matrix of the $U(\Omega)$ function at the solution.[31] It should be noted that the uncertainties reported in Table 3 do not take into account the strong correlations (correlation coefficients >0.9) that were found between the c20 and c40 coefficients for site 44 and between c22 and c44 for site 69.

Calculation of HF-EPR Spectra. HF-EPR spectra were calculated using the diffusion tilt angles and c_K^L coefficients obtained from the MD trajectories, which were fixed at the values given in Table 2 and Table 3. The rotational rates R_x, R_y, and R_z were varied to fit the experimental spectrum using nonlinear least-squares.[10] The magnetic parameters used in the slow-motional fits were slightly different for the two sites; the values obtained from least-squares fitting of the rigid limit spectra from ref 1 are given in Table 4. An isotropic Lorentzian line width (derivative peak-to-peak) of 0.6 mT was used for both sites.

Figure 7 directly compares experimental spectra for label sites 44 and 69 obtained at 283 K to the spectra calculated in this way. The optimal values of the rotational diffusion constants in the fits were $\log_{10} R_x \cdot \text{sec} = 7.44$, $\log_{10} R_y \cdot \text{sec} = 8.47$, $\log_{10} R_z \cdot \text{sec} = 8.11$ for site 44, and $\log_{10} R_x \cdot \text{sec} = 7.16$, $\log_{10} R_y \cdot \text{sec} = 8.86$, $\log_{10} R_z \cdot \text{sec} = 7.73$ for site 69.

TABLE 4: Magnetic Parameters Used for MTSSL Spin Labels at Sites 44 and 69 on T4 Lysozyme

site	g_{xx}	g_{yy}	g_{zz}	A_x (mT)	A_{yy} (mT)	A_{zz} (mT)
44	2.0078	2.0057	2.0022	0.62	0.57	35.8
69	2.0077	2.0056	2.0022	0.64	0.61	35.4

Discussion

The hybrid method presented here for combining MD and SLE simulations to predict EPR spectra has a number of advantages over trajectory-based methods for analyzing the dynamics of nitroxide spin labels attached to biomolecules. Many of these advantages derive from the fact that the MD trajectory is parametrized according to the spin label diffusion properties in this method. This affords a concise characterization of the label motion that can be directly compared with parameters obtained from least-squares analysis of the slow-motional EPR line shape. A particularly useful feature of this approach is that the molecular structure of the protein and label can be related directly to the axes that define the label motion, providing new physical insights into the label's dynamic behavior and interaction with its surroundings.

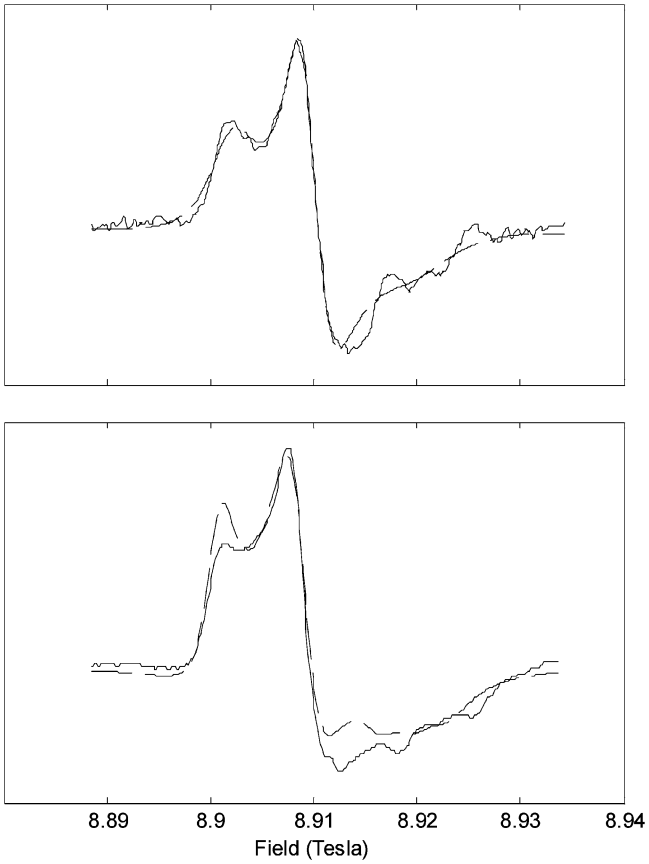

Figure 7. Comparison of experimental (solid lines) and calculated (dashed lines) 250 GHz spectra for a nitroxide label at site 44 (a) and site 69 (b) of T4 lysozyme at 10 C.

Because the diffusion parameters from the MD dynamics can be used directly to calculate a slow-motional EPR line shape, the MD results can also be used to guide line shape analysis of experimental spectra. That is, by providing limits on the range of parameters to be searched in a least-squares minimization, this approach can resolve possible ambiguities and uncertainties that may arise from least-squares determination of these parameters. The MD also reveals details of the label diffusion that may not be resolvable by line shape analysis alone, including the full anisotropy of the rotational diffusion, all of the diffusion tilt angles, and higher-order terms in the orienting potential that may reflect irregular orientational distributions of the label.

Finally, the diffusion operator approach described here is considerably faster than previous trajectory-based methods for calculating the EPR spectrum, which greatly aids analysis of experimental results and may enable one to iteratively refine molecular models of spin-labeled proteins using their EPR spectrum.

Comparison with Experiment. The accuracy of any predictive technique is ultimately validated by the quality of its fits to the experimental spectra. The use of high field spectra to verify predictions based on MD results presents an additional challenge relative to X-band spectra, which because of their lower spectral resolution do not demand accuracy of the rotational diffusion tensor, tilt angles, and ordering potential coefficients.

As can be seen in Figure 7 the overall features of the 250 GHz line shapes are generally quite well-reproduced by the MD-based line shapes for both label sites studied, representing a dramatic improvement over previous attempts to reproduce 250 GHz spectra from MD trajectories.[9] However, some discrepancies between the calculated and predicted spectra are apparent in Figure 7, particularly near the high- and low-field extremes of the spectrum for site 69. It is important to note that reasonably good agreement was achieved by *varying only the principal diffusion tensor rates* and retaining all the other information about tilt angles and ordering obtained directly from the MD simulations.

In fact, we found that considerable improvement in the fits could be achieved by varying the other diffusion parameters (particularly the orienting potential coefficients) within the uncertainty bounds obtained from the MD analysis (cf. Table 3 and accompanying discussion). In their original analysis of these 250 GHz spectra Barnes et al.[1] could only achieve satisfactory agreement with the experimental spectra at both label sites by including a second species of label with different mobility and slightly different magnetic parameters, based on evidence for such a species from 9 GHz spectra. Inclusion of a second species with different mobility would certainly improve the fit to the experimental line shape in the present case as well. Indeed, our simulations do predict bimodal orientational distributions within the same site (cf. Figure 6) although we found no evidence was found for different label mobilities between the two modes. We discuss below how fits to experimental spectra might be further improved within the context of a more conservative one-site model that nevertheless could reproduce some of the features of two site models. However, these considerations are secondary to the main point that the parameters predicted from the MD agree quite well with the experimental spectra without requiring further adjustment.

One drawback of attempting to refine all of the available diffusion parameters of the label by least-squares analysis of experimental spectra is that there are too many parameters in the full model to permit an unambiguous solution. As noted above, parametrization of the MD trajectory, and in particular the estimated uncertainties in the parameters, offer a useful guide for line shape analysis by establishing boundaries for the least-squares parameter search. This is illustrated in Figure 8, which shows the range of line shapes corresponding to the uncertainty bounds of the c_0^2 potential coefficient. The dashed lines indicate spectra calculated with c_0^2 at the lower limit of the uncertainty region indicated in Table 3, and the dotted lines show spectra calculated with c_0^2 at the upper limit, holding all other parameters at their given values. (The dotted line closely overlaps the solid line in Figure 8a, and is not clearly visible.) By limiting the range of solution for some of the fitting parameters in this way, it is possible to obtain values for other parameters as well, leading to a substantially more detailed picture of the probe motion.

Rotational Diffusion Principal Axes. The analysis of the MD trajectories presented here provides considerably more detail about the rotational diffusion of the spin label than has previously been reported for trajectory-based calculations; in particular, the rotational diffusion tilt angles are fully determined by this method.

Although knowledge of the principal rotational diffusion axes of a nitroxide label is not necessary to calculate its slow-motional EPR spectrum using trajectory methods, any quantitative comparison of dynamics from the molecular model with experimental spectra does require assignment of the diffusion axes so that rotational correlation times may be calculated. Most MD treatments in the literature have simply assumed that the rotational diffusion axes coincide with the magnetic axes[2−5,26] (this assumption did not affect the results of Steinhoff and co-

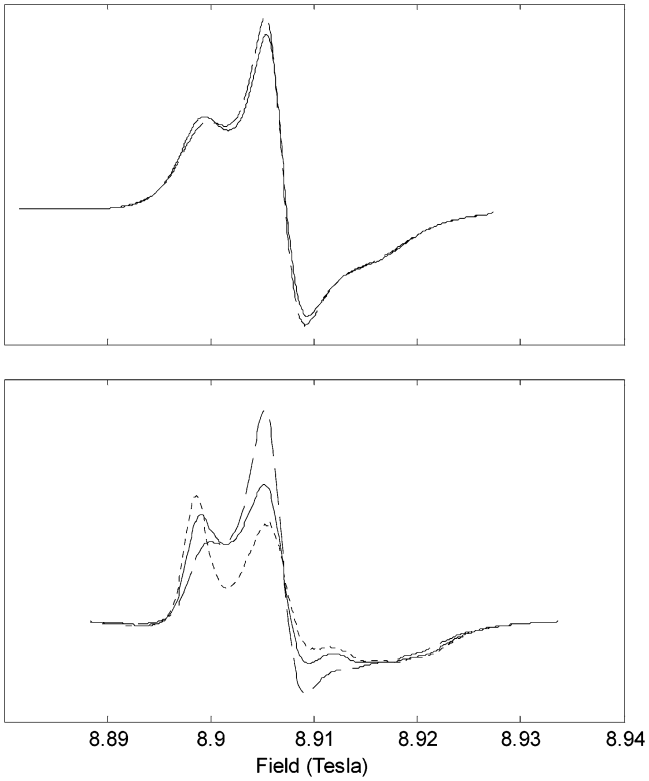

Figure 8. Sensitivity of calculated 250 GHz spectra to the c_0^2 potential coefficient for nitroxide labels at site 44 (a) and site 69 (b) of T4 lysozyme at 10 C. Solid lines show best-fit line shapes as in Figure 7 calculated with c_0^2 coefficient given in Table 3. Line shapes calculated with c_0^2 at the lower limit of the uncertainty region indicated in Table 3 are shown with dashed lines, and those with c_0^2 at the upper limit are shown with dotted lines. The dotted line is not visible in part (a) because it closely overlaps the solid line.

workers, who also assumed an isotropic rotational correlation time for all label sites on bacteriorhodopsin.[3,5]) Although this assumption appears to yield reasonable agreement with experimental spectra at X-band, higher-frequency spectra are very sensitive to both the anisotropy and the principal axis directions of the rotational diffusion tensor,[32] and accurate determination of these quantities is essential to achieve good agreement between the MD results and experimental EPR spectra.

For both probe locations investigated, we found that the axis of fastest rotation ($\mathbf{z}_R$) of the spin label lies closest to the direction of the N−O bond. This result differs significantly from the assumptions of previous MD calculations but is somewhat more consistent with the tilt angles obtained by least-squares analysis of experimental line shapes at 9 and 250 GHz.[1,24,30] The results suggest that the fastest rotation of the label occurs around the axis of the first tether bond, i.e., the χ_5 torsional angle.

In contrast to the conclusion of Steinhoff and co-workers based upon X-band results,[3,5] our high-frequency results also demonstrate that the spin label rotational diffusion can be quite anisotropic, with significantly different rate constants for the $\mathbf{x}_R$, $\mathbf{y}_R$, and $\mathbf{z}_R$ axes. Such anisotropy is consistent with the constraints imposed by the covalent tether of the nitroxide label. Determination of the rotation rates for the individual axes (and their temperature dependences) thus offers new insights into the nature of the interactions between the label and its surroundings.

Director Axis. As was the case for the principal diffusion axes, it is not necessary to determine the local director to calculate an EPR spectrum using trajectory-based methods; however, quantitative comparison of label orientation between the MD calculation and experimental results does require the director orientation. Typically, the S_{20} order parameter is used to characterize ordering:

$$S_{20} = \frac{1}{2}\langle 3\cos^2\theta - 1\rangle$$

where θ is the angle between the director and a given axis in the label frame (cf. eq 7). Two groups have reported a comparison of order parameters obtained from MD and from experiment. LaConte et al.[26] assumed the director to be the mode of the $\mathbf{z}_R$ distribution, that is, the orientation visited most often by the $\mathbf{z}_R$ axis over the trajectory, whereas Stoica[9] made such a comparison without explicitly defining the director orientation.

Figure 9 demonstrates the discrepancies that can arise among the various possible definitions for the director orientation. Shown in this figure is the temperature dependence of the diffusion z ($\mathbf{z}_R$) axis orientation distribution in the protein frame. At the lowest temperature, 275 K, $\mathbf{z}_R$ appears to fluctuate around a single orientation. As the temperature is raised, a second, less intense spot appears, corresponding to another major orientation with slightly higher potential energy. As the temperature is increased above 300 K, the second spot becomes more intense, reflecting increased thermal population of the higher-energy orientation. At the highest temperature studied, 400 K, the spots are nearly equal in intensity. This behavior suggests the presence of two minima in the orienting potential with different energies, such that the orientation corresponding to the higher-energy minimum is only thermally populated at higher temperatures. The observed distribution is also consistent with the bimodal distribution observed in the χ_5 torsional angle (cf. Figure 4) and suggests that the two orientations correspond to the trans and gauche configurations around the first tether bond.

The observed bimodal distribution leads to discrepancies between different definitions of the director as follows. The mode of $\mathbf{z}_R$, which corresponds to the point of darkest intensity on the larger spot at each temperature in Figure 9, is essentially independent of temperature over the range studied. However, the direction determined by diagonalizing the order matrix (cf. Methods) is significantly temperature-dependent: at the lowest temperature, the director appears at an orientation near the mode of $\mathbf{z}_R$ at the center of the more populated energy minimum but moves toward a position between the two minima as the second major orientation becomes more heavily weighted at higher temperatures. Similar temperature behavior was observed in the $\mathbf{z}_R$ distributions and director orientations for the label at residue 44.

Our results demonstrate the importance of determining the direction of the director axis relative to the protein structure. Different choices for the director axis can lead to significantly different effective potential coefficients for the same physical distribution of label orientations. Perhaps more significantly, the director orientation provides a useful physical picture of the interactions between the label and the protein. For example, it has been suggested that that the steric restrictions on the motional amplitude of a label are the major determinant of its EPR spectrum, whereas its rate of motion has a relatively minor effect.[3] If nonbonding interactions are the dominant influence on label orientation, one might expect the director axis to lie along the approximate symmetry axis of the cavity surrounding the label. However, the orientation of the director for both label sites analyzed (cf. Figure 5) suggests that the tether bond plays at least as great a role in determining the orientation distribution of the nitroxide.

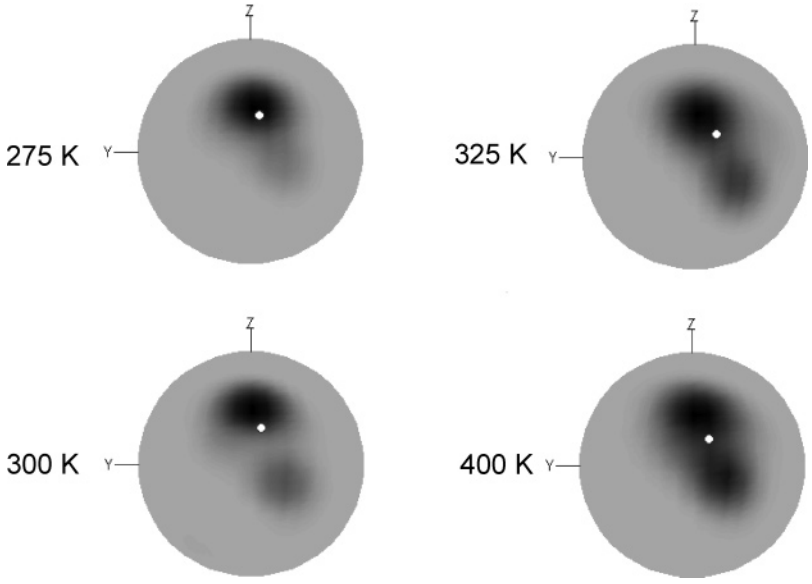

Figure 9. Intensity plots on the unit sphere surface showing the orientation distribution of the nitroxide diffusion *z* (z_R) axis in the protein frame for T4 lysozyme labeled at residue 69 at four temperatures. The director orientation calculated from the ordering matrix for each distribution is shown by a white dot.

Ordering Potential. The diffusion operator SLE method can also provide new details about the physical constraints placed on the motion of the tethered label. Depending on the degree to which steric interactions with neighboring residues contribute to the label's orientation distribution, these constraints may be expected to be appreciably asymmetric. Results from published BD and MD calculations have generally been interpreted in terms of simple symmetric distributions such as the "cone" model.[5,26] Although simple orientational distributions can lead to satisfactory (but not perfect) agreement with experimental X-band spectra, they are insufficient for the higher orientation resolution available with HF-EPR. The approach introduced by Steinhoff and Hubbell[3] wherein an orienting potential is represented using multiple Gaussian distributions in the rotation angles can accommodate complex, asymmetric orientation distributions. An alternative approach within the context of available SLE programs is to include higher-order terms such as c_0,$^4c_2$,^{4} and $c_4{}^4$ in the orienting potential to account for irregularities in the shape of the probe orientational distribution.

Despite the availability of higher-order terms in the orienting potential, the expansion given in eq 1 still has some significant limitations. The first and most obvious one is that the restriction to terms having $L,K = 2$ or 4 means that the resulting potential will have 2- or 4-fold symmetry, which may not be realized in practical systems. Thus, for example, the bimodal distribution shown in Figure 9 can be represented by eq 1 for the indicated director orientations only at the lowest temperature and in the high-temperature limit, where the distributions have 2-fold or higher symmetry with respect to the director. In the intermediate cases where the MD results show two unequally populated modes, the best-fit coefficients yield either a single, elongated orientation distribution or a symmetric, bimodal distribution with the average population in each mode.

A second, more subtle limitation of the orienting potential expansion in eq 1 is that it assumes the principal axes of the orientation distribution coincide with the principal diffusion axes. It does not appear to have been generally appreciated in previous comparisons of MD and EPR results that the magnitude of S_{20} depends on which axis in the nitroxide frame is used to calculate it. Reported S_{20} values have been calculated with reference to the $\mathbf{z}_M$ axis of the nitroxide,[9,26] even though the principal diffusion axis is closest to $\mathbf{x}_M$ and yields significantly different S_{20}. values from $\mathbf{z}_M$.

More rigorously, one may define a set of ordering axes in the label frame by diagonalizing the order matrix calculated in this frame relative to the director according to the procedure of Zannoni.[27] In our MD simulations, the principal ordering axes obtained in this way did differ significantly from the principal rotation axes of the label. This finding can be rationalized for the case of a covalently tethered label: whereas the rotational diffusion tensor is primarily determined by rotation of the label around its tether bonds, the local ordering also reflects steric interactions with surrounding side groups, which may have a different orientation dependence. Because of the limitations of the present SLE line shape calculation, we have neglected any tilt between the two axis systems, although this assumption is not inherent to the diffusion operator approach described here.

In summary, the most accurate representation of the orientation distribution obtained from MD in terms of diffusion parameters requires both the asymmetric character of the distribution and possible tilt between the ordering and the principal diffusion axes to be taken into account. This could be accomplished by including a complete set of functions in the potential function expansion (i.e., odd L and K indices and antisymmetric as well as symmetric combinations of $\mathbf{D}^L_{MK}(\Omega)$ and $\mathbf{D}^L_{M,-K}(\Omega)$). The distribution could in principle be represented to arbitrarily high precision by including additional terms in the expansion of the orienting potential function. Such a generalized potential would enable one to represent asymmetric or multimodal label distributions such as those shown in Figure 9 without having to include additional "sites" or species in the line shape analysis of experimental spectra.

Comparison with Trajectory-Based Methods. The diffusion operator parametrization method presented in this work is significantly less computationally demanding than the trajectory methods that have been previously applied to EPR spectral simulation. As noted in the seminal work of Robinson et al.[2] it is necessary to calculate trajectories of sufficient length to provide adequate spectral resolution; for example, trajectories with 2^{14} (16 384) points were needed to achieve 0.3 G resolution. Moreover, averaging over initial orientation required 4000

trajectories. In the absence of an orienting potential, this could be reduced to 40 trajectories using sampling methods,[2] although this case does not apply to more complex systems such as spin-labeled proteins. The "direct" MD method applied by Håkansson et al. to spin-labeled lipids utilized a 100 ns MD trajectory (5×10^7 steps) but also extrapolated the free induction decay (FID) signal to 600 ns using a fit to the orientational correlation function from the MD simulation.[6] This procedure was used to obtain 9 GHz EPR spectra in the incipient fast-motion regime. For slow motions at high EPR frequencies, the computational demands become significantly greater: for example, Stoica[9] employed 10 trajectories of 5.5−6.0 ns each ($\sim 2.8 \times 10^7$ steps) but failed to produce any reasonable agreement with experimental 250 GHz spectra of labeled T4 lysozyme, underlining the difficulties remaining with this approach.

In the diffusion operator approach, the time-consuming MD is used only to determine the local steric constraints experienced by the label, and not to calculate the EPR spectrum itself. This advantage is particularly significant for HF EPR spectra, for two reasons: first, the time required to carry out a SLE-based line shape calculation depends less strongly on frequency than orientation-sampling methods,[12] and second because less MD time is required to simulate dynamics on the shorter time scales to which HF EPR is sensitive. Carrying out MD simulations at a higher equilibrium temperature and scaling the resulting potential coefficients to the desired k_bT could achieve further reduction in computation time.

Limitations of the Diffusion Operator Approach. We conclude by briefly considering some of the limitations of the diffusion operator approach for simulating slow-motional EPR spectra by MD. As has been pointed out by Robinson et al.[2] and Westlund and co-workers,[5] the SLE method is restricted to a specific model of diffusion that is determined by the diffusion operators used. In contrast, trajectories from MD calculations are not tied to any specific motional model, although it has been observed that the dynamics can depend significantly on the force field employed.[9] One model dependent aspect of currently available SLE programs arises from the assumptions underlying the specific form that is utilized for the orienting potential (eq 1). As noted above, the diffusion operator can be made significantly more flexible by generalizing the orienting potential used to fit the MD results. The heuristic approach of optimizing the director and principal diffusion axis directions also avoids model-dependent assumptions.

A potentially more serious limitation is that simple diffusion operators cannot adequately represent compound motion, for example, the combined effects of slow domain motion or overall tumbling of the protein with the fast librational motion of the spin label. One approach to solving this problem within the context of SLE calculations is the Slowly Relaxing Local Structure (SRLS) model of Polimeno and Freed.[13] To estimate all of the parameters in the SRLS model using MD would require adequate sampling of the long-time scale protein motions, which would in turn necessitate trajectories similar in length to those needed for direct MD calculations. These considerations suggest that the most effective application of the diffusion operator parametrization method is to provide an independent characterization of the local label dynamics, so that the domain and overall protein motion can be separately determined by multifrequency EPR.

Conclusion

We have presented a new method to calculate slow-motional EPR spectra of a spin-labeled biomolecules from molecular dynamics by parametrizing the motion in the MD trajectories and using the resulting parameters as inputs to SLE-based line shape simulations. The method greatly improves the efficiency of the EPR line shape calculation over previous trajectory-based methods, and is equally applicable to high and low EPR frequencies. The method should prove particularly advantageous for computationally demanding high-field EPR simulations, and reasonable agreement with experimental 250 GHz spectra was demonstrated. An important feature of the method is that it allows detailed determination of the rotational tensor anisotropy, diffusion tilt angles, and higher-order orientational ordering effects. Moreover, these quantities are related directly to the molecular structure of the labeled protein, offering useful physical insights into the protein and probe dynamics. In the future, accounting for the local probe motion using this approach will allow one to deconvolute librational motion from the complex EPR spectra to obtain the domain motion that is often of biological interest. With reasonable optimization, the approach described here should be efficient enough to enable direct iterative refinement of molecular models based on least-squares fitting of experimental EPR spectra.

Acknowledgment. This work was supported by National Science Foundation grants MCB 960094 (D.E.B.) and MCB-0346650 (P.G.F), and an IHRP grant from the National High Magnetic Field Laboratory. We gratefully acknowledge Prof. Bruce Robinson for several useful discussions.

References and Notes

(1) Barnes, J. P.; Liang, Z.; Mchaourab, H. S.; Freed, J. H.; Hubbell, W. L. *Biophys. J.* **1999**, *76*, 3298.
(2) Robinson, B. H.; Slutsky, L. J.; Auteri, F. P. *J. Chem. Phys.* **1992**, *96*, 2609.
(3) Steinhoff, H. J.; Hubbell, W. L. *Biophys. J.* **1996**, *71*, 2201.
(4) Steinhoff, H.-J.; Müller, M.; Beier, C.; Pfeiffer, M. *J. Mol. Liq.* **2000**, *84*, 12.
(5) Usova, N.; Westlund, P. O.; Fedchenia, I. I. *J. Chem. Phys.* **1995**, *103*, 96.
(6) Hakansson, P.; Westlund, P. O.; Lindahl, E.; Edholm, O. *Phys. Chem. Chem. Phys.* **2001**, *3*, 5311.
(7) Steinhoff, H.-J.; Hubbell, W. L. *Biophys. J.* **1996**, *71*, 2201.
(8) Steinhoff, H.-J.; Müller, M.; Beier, C.; Pfeiffer, M. *J. Mol. Liq.* **2000**, *84*, 17.
(9) Stoica, I. *J. Phys. Chem. B* **2004**, *108*, 1771.
(10) Budil, D. E.; Lee, S.; Saxena, S.; Freed, J. H. *J. Magn. Reson.* **1996**, *120*, 155.
(11) Freed, J. H. Theory of Slow Tumbling ESR Spectra for Nitroxides. In *Spin Labeling Theory and Applications*, 1st ed.; Berliner, L. J., Ed.; Academic Press: New York, 1976; Vol. 1, p 53.
(12) *Calculating Slow Motional Magnetic Resonance Spectra*; Schneider, D. J., Freed, J. H., Eds.; Plenum Press: New York and London, 1989; Vol. 8, pp 1.
(13) Polimeno, A.; Freed, J. H. *J. Phys. Chem.* **1995**, *99*, 10995.
(14) Matsumura, M.; Wozniak, J. A.; Sun, D. P.; Matthews, B. W. *J. Biol. Chem.* **1989**, *264*, 16059.
(15) Sale, K.; Sar, C.; Sharp, K. A.; Hideg, K.; Fajer, P. G. *J. Magn. Reson.* **2002**, *156*, 104.
(16) Lajzerowicz-Bonneteau, J. Molecular structures of nitroxides. In *Spin Labeling: Theory and Applications*; Berliner, L. J., Ed.; Academic Press: New York, 1976; p 239.
(17) Barone, V.; Capecchi, G.; Brunel, Y.; Andries, M.-L. D.; Subra, R. *J. Comput. Chem.* **1997**, *18*, 1720.
(18) Barone, V.; Bencini, A.; Cossi, M.; Di Matteo, A.; Mattesini, M.; Totti, F. *J. Am. Chem. Soc.* **1998**, *120*, 7069.
(19) Brooks, B. R.; Bruccoleri, R. E.; Olafson, B. D.; States, D. J.; Swaminathan, S.; Karplus, M. *J. Comput. Chem.* **1983**, *4*, 187.
(20) Chang, G.; Guida, W. C.; Still, W. C. *J. Am. Chem. Soc.* **1989**, *111*, 4379.
(21) Li, Z.; Scheraga, H. *Proc. Natl. Acad. Sci. U.S.A.* **1987**, *84*, 6611.
(22) Ripoll, D. R.; Scheraga, H. A. *Biopolymers* **1988**, *27*, 1283.
(23) Zare, R. N. *Angular Momentum: Understanding Spatial Aspects in Chemistry and Physics*; John Wiley and Sons: New York, 1988.
(24) Colombus, L.; Kálai, T.; Jekö, J.; Hideg, K.; Hubbell, W. L. *Biochemistry* **2001**, *40*, 3828.

(25) Meirovitch, E.; Igner, D.; Igner, E.; Moro, G.; Freed, J. H. *J. Chem. Phys.* **1982**, *77*, 3915.
(26) LaConte, L. E.; Voelz, V.; Nelson, W.; Enz, M.; Thomas, D. D. *Biophys. J.* **2002**, *83*, 1854.
(27) Zannoni, C. Distribution functions and order parameters. In *The Molecular Physics of Liquid Crystals*; Luckhurst, G. R., Gray, G. W., Eds.; Academic Press: New York, 1979; p 51.
(28) Saupe, A. *Angew. Chem., Int. Ed. Engl.* **1968**, *7*, 97.
(29) Lagarias, J. C.; Reeds, J. A.; Wright, M. H.; Wright, P. E. *SIAM J. Optimization* **1998**, *9*, 112.
(30) Langen, R.; Oh, K. J.; Casicio, D.; Hubbell, W. *Biochemistry* **2000**, *39*, 8396.
(31) Seber, G. A. F.; Wild, C. J. *Nonlinear Regression*; Wiley-Interscience: New York, 1989.
(32) Budil, D. E.; Earle, K. A.; Freed, J. H. *J. Phys. Chem.* **1993**, *97*, 1294.